



# Hydrothermal synthesis of $\beta$ -nickel hydroxide nanocrystalline thin film and growth of oriented carbon nanofibers

Enlei Zhang<sup>a</sup>, Yuanhong Tang<sup>a,b,\*</sup>, Yong Zhang<sup>a</sup>, Chi Guo<sup>a</sup>, Lei Yang<sup>a</sup>

<sup>a</sup> College of Materials Science and Engineering, Hunan University, Changsha 410082, People's Republic of China

<sup>b</sup> Powder Metallurgy Research Institute, Central South University, Changsha 410083, People's Republic of China

## ARTICLE INFO

### Article history:

Received 13 October 2008

Received in revised form 5 March 2009

Accepted 12 March 2009

Available online 25 March 2009

### Keywords:

- A. Thin films
- B. Chemical synthesis
- C. X-ray diffraction
- D. Catalytic properties

## ABSTRACT

Novel well-crystallized  $\beta$ -nickel hydroxide nanocrystalline thin films were successfully synthesized at low temperature on the quartz substrates by hydrothermal method, and the oriented carbon nanofibers (CNFs) were prepared by acetylene cracking at 750 °C on thin film as the catalyst precursor. High resolution transmission electron microscopy (HR-TEM) measurement shows that thin films were constructed mainly with hexagonal  $\beta$ -nickel hydroxide nanosheets. The average diameter of the nanosheets was about 80 nm and thickness about 15 nm. Hydrothermal temperature played an important role in the film growth process, influencing the morphologies and catalytic activity of the Ni catalysts. Ni thin films with high catalytic activity were obtained by reduction of these Ni(OH)<sub>2</sub> nanocrystalline thin films synthesized at 170 °C for 2 h in hydrothermal condition. The highest carbon yield was 1182%, and was significantly higher than the value of the catalyst precursor which was previously reported as the carbon yield (398%) for Ni catalysts. The morphology and growth mechanism of oriented CNFs were also studied finally.

© 2009 Elsevier Ltd. All rights reserved.

## 1. Introduction

Among transition metal hydroxides, nickel hydroxide (Ni(OH)<sub>2</sub>) has been of particular interest for its importance in fundamental researches and potential applications in catalysis, electronic and magnetic fields [1–9]. As inspired by both the potential application of Ni(OH)<sub>2</sub> and the novel properties of nanoscale materials, considerable works have been done to understand the structure and electrochemical properties of zero- and one-dimensional nickel hydroxide, but little attention was paid to the usage of two-dimensional nickel hydroxide nanoscale materials as catalyst precursors. It is well known that Ni-based catalysts were extensively studied due to their relatively higher activities compared with other transition metals [10–12]. Because the catalytic activity of the Ni catalysts decreased with time on stream due to the continuous deposition of carbon, the effective catalysts should exhibit sufficient carbon storage capacity on a per-gram basis of nickel, in addition to reasonable activity toward carbon source decomposition at relatively lower temperatures [13,14]. And nickel hydroxide has been regarded as the most important

intermediate during the synthesis of nickel oxide and metal nickel. Therefore, nanostructured Ni(OH)<sub>2</sub> nanocrystalline thin films are highly desired. Now a variety of physical as well as chemical methods have been applied for the deposition of metal thin films, namely, pulsed laser deposition, sputtering, dip coating process, spray pyrolysis, electrodeposition, etc. [15–23]. But these methods had many drawbacks such as small area of deposition, requirement of sophisticated instruments, high working cost of system, high deposition temperature, wastage of depositing material, cleaning after each deposition, etc. Thus, seeking simple, easily controlled methods to synthesize Ni(OH)<sub>2</sub> nanocrystalline thin film is still a hotspot of researchers.

By comparing with other methods, the hydrothermal method not only helps in processing monodispersed and highly homogeneous nanoparticles, but also acts as one of the most attractive techniques for processing thin films. The hydrothermal method is ideal for the processing of very fine nanocrystalline thin films having high purity, controlled stoichiometry, high quality, narrow particle size distribution, controlled morphology, high crystallinity and so on because of the highly controlled diffusivity in a strong solvent media in a closed system [24–26].

In this paper, we report a simple method to directly synthesize  $\beta$ -Ni(OH)<sub>2</sub> nanocrystalline thin films under hydrothermal conditions. The influence of experimental conditions and structure of as obtained thin films have been systemically investigated. Moreover, we found that Ni thin films with high catalytic activity were

\* Corresponding author at: College of Materials Science and Engineering, Hunan University, Changsha, Hunan 410082, P. R. China. Tel.: +86 7318821778; fax: +86 7318821778.

E-mail address: [yhtang2000@163.com](mailto:yhtang2000@163.com) (Y.H. Tang).

obtained by reduction of these Ni(OH)<sub>2</sub> nanocrystalline thin films synthesized with the hydrothermal method, and the oriented carbon nanofibers were formed on the Ni thin films by cracking acetylene.

## 2. Experimental

All of the chemicals were of analytical grade and used without further purification. In a typical procedure, 0.1 M solution of NiSO<sub>4</sub>·6H<sub>2</sub>O was taken in the 1:2 stoichiometric molar ratio along with 20% solution of NaOH. NiSO<sub>4</sub>·6H<sub>2</sub>O immediately reacted with the NaOH in the solution to form Ni(OH)<sub>2</sub>. The mixed solution (250 ml) was transferred into a stainless steel autoclave of capacity (1000 ml). Then, a quartz substrate (5 mm × 5 mm × 2 mm) was put into the autoclave. After the autoclave was sealed, then heated to 100–300 °C, 1.8–11 MPa of pressure were maintained for several hours. Finally, the autoclave was cooled naturally. The light green film was firmly formed on the surface of the substrate. The product was washed by distilled water for several times to remove excess salts, and then dried at 80 °C overnight in air.

The catalytic activity of β-Ni(OH)<sub>2</sub> was tested by the degree of acetylene conversion, C<sub>2</sub>H<sub>2</sub> → 2C + H<sub>2</sub>. The β-Ni(OH)<sub>2</sub> thin film and powder were placed in a quartz boat and were then introduced into a chamber of a tube furnace. The quartz boat was heated to 400 °C at a rate of 10 °C min<sup>-1</sup> under vacuum and then reduced at 400 °C for 2 h in a flow of 9% hydrogen in argon under atmospheric pressure. Subsequently, a flow of 9% acetylene in argon was introduced into the chamber at a flow rate of 100 sccm, oriented CNFs were formed on the thin film by deposition of carbon atoms from decomposition of acetylene at 700 °C for 1 h. The percentage of carbon yield is defined as follows [27–29]:

$$\text{carbon yield}(\%) = 100 \times \frac{\text{weight of carbon deposited on the catalyst}}{\text{weight of the catalyst}} \quad (1)$$

The synthesized samples were characterized by X-ray diffraction (XRD) using the Siemens D 5000 diffractometer with Cu Kα radiation (λ = 1.54178 Å). Morphology observation of β-Ni(OH)<sub>2</sub> thin film and oriented CNFs was performed with field emission transmission electron microscopy (SEM, JEOL JSM-5600LV), high resolution transmission electron microscopy (HR-TEM, JEOL JEM-3010). Thermogravimetric (TG) data and differential scanning calorimetry (DSC) curves were obtained at a heating rate of 10 °C min<sup>-1</sup> in nitrogen by thermal analyzer (Netzsch STA449C).

## 3. Results and discussion

Hydrothermal temperature is one of the most important factors to influence the film features, since the nucleation and growth processes of Ni(OH)<sub>2</sub> are determined by the hydrothermal temperature. The crystal phase and structure information of the thin films were obtained by XRD measurements. Fig. 1 shows the XRD pattern of the Ni(OH)<sub>2</sub> thin films deposited with various hydrothermal temperatures. One of the phase is indexed to the (0 0 1), (1 0 0), (1 0 1), and (1 0 2) planes of β-Ni(OH)<sub>2</sub> (JCPDS no.

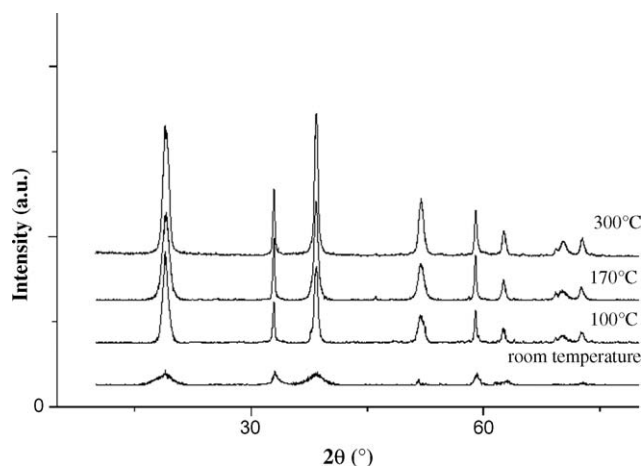


Fig. 1. XRD patterns of the as-received samples with different temperatures.

14-0117) displaying a hexagonal lattice ( $a = 3.12 \text{ \AA}$  and  $c = 4.62 \text{ \AA}$ ) with the typical peaks at  $2\theta = 19.25^\circ$ ,  $33.06^\circ$ ,  $38.54^\circ$ , and  $52.1^\circ$ , respectively [30,31]. It proves that the thin film with β-Ni(OH)<sub>2</sub> has deposited on the substrate. Crystalline sizes presented in Table 1 were calculated using the Scherrer equation.

$$D_{hkl} = \frac{K\lambda}{\beta_{hkl} \cos \theta} \quad (2)$$

where  $D_{hkl}$  is the crystalline size along the  $[h k l]$  direction,  $\beta_{hkl}$  is the fwhm of a given  $[h k l]$  peak, and  $K$  is the structure factor. The diffraction peaks are gradually becoming narrower and crystal size larger with increasing hydrothermal temperature to 170 °C, indicating the growth of β-Ni(OH)<sub>2</sub> crystalline, as shown in Table 1. The width of peaks also indicates that the particles size is of the nanometer scale. With increasing the hydrothermal temperature from 170 to 300 °C, the diffraction peaks and average size of β-Ni(OH)<sub>2</sub> crystallites are not varied obviously.

Fig. 2 clearly reveals the morphologies of the nanostructure β-Ni(OH)<sub>2</sub> thin films deposited on the quartz substrates under different hydrothermal temperatures and time. The thickness of the films was about 100 nm. At room temperature (Fig. 2a), a few sheets were obtained with poorly crystallized structure and more irregular shape. When the temperature increased to 170 °C (Fig. 2b), well-crystalline hexagonal structure nanosheets were observed, and the nanosheet had the small face diameter of about 80 nm. Then further increasing the hydrothermal temperature and time (Fig. 2c and d), structure and crystalline size of β-Ni(OH)<sub>2</sub> nanosheets were not varied obviously, indicating that the formation process was almost complete. It is in a good agreement with the result of XRD. It is seen from Fig. 2e that the β-Ni(OH)<sub>2</sub> nanosheets obviously exhibit the preferred orientation along the direction perpendicular to the substrate, and the nanosheets are homogeneous, displaying a hexagonal structure. It is well known that the β-Ni(OH)<sub>2</sub> possesses the typical CdI<sub>2</sub> structure [32], which is layered structure, so formed M(OH)<sub>2</sub> nanosheets are stable

Table 1  
Effect of different hydrothermal conditions on the catalytic activity of β-Ni(OH)<sub>2</sub> samples.

Sample	Temperature (°C)	Time (h)	Pressure (MPa)	Crystalline size (nm)		Yield of CNFs (wt.%)
				Face diameter	Thickness	
S1	Room temperature	2	Atmosphere	15	10	177
S2	100	2	0.3	75	15	494
S3	170	2	2	80	16	1822
S4	300	2	9.4	85	15	1611
S5	170	8	2	80	16	1258

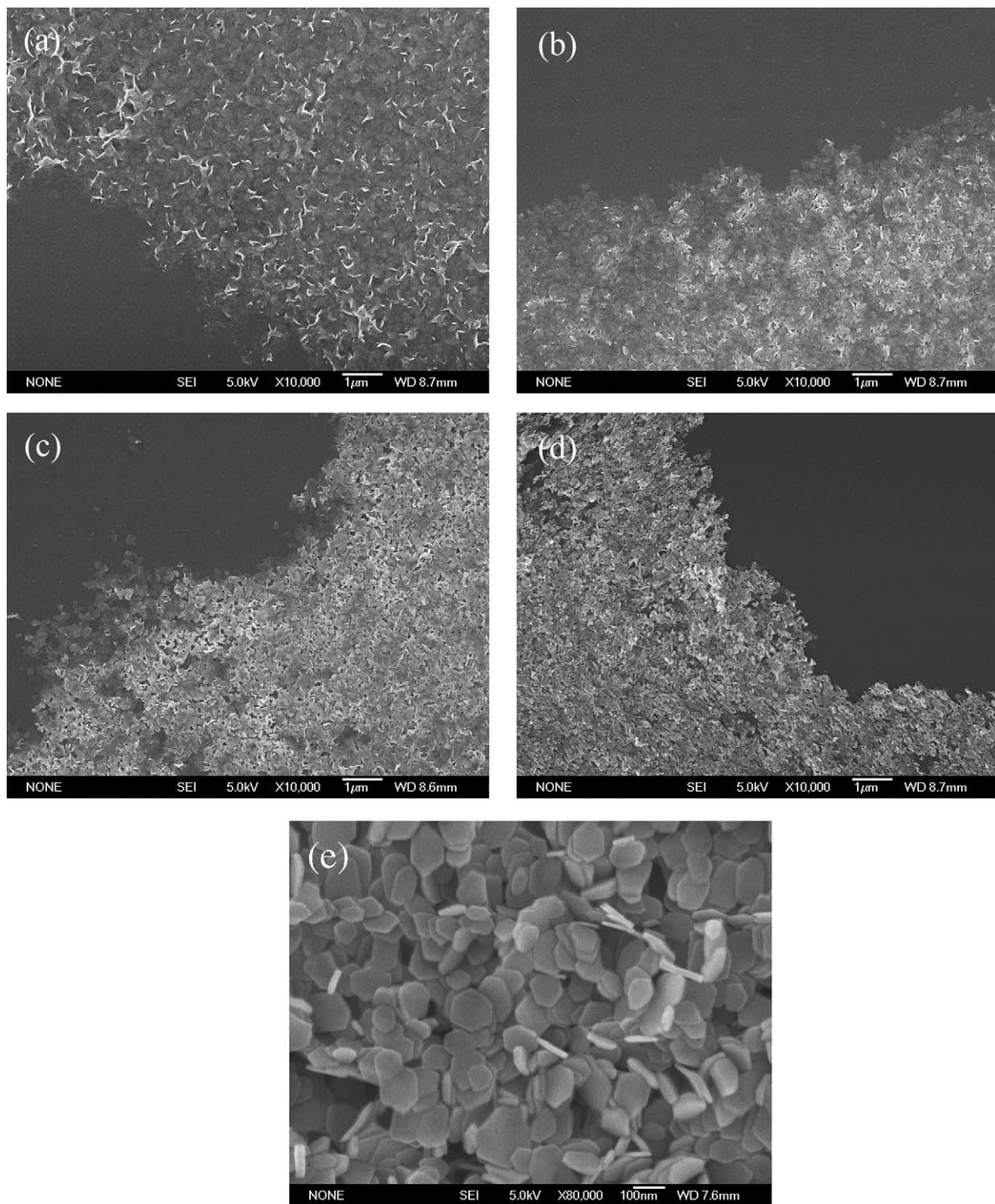


**Fig. 2.** SEM images of samples synthesized by different hydrothermal conditions. (a) S1; (b) S3; (c) S4; (d) S5. (e) The magnified SEM image of S3.

geometrical morphologies in the surface chemistry context, because with sheet shapes  $M(OH)_2$  have a low system energy. These sheet-like nuclei aggregate together under hydrothermal condition, and then they grow up, and the slurry dissolves gradually. At the same time, the nucleation takes place on the substrate, which leads to the growth of  $Ni(OH)_2$  nanosheets to construct  $Ni(OH)_2$  thin film.

The TEM images of  $\beta-Ni(OH)_2$  nanosheets prepared at 170 °C for 2 h are shown in Fig. 3. TEM image (Fig. 3a) underlines not only the homogeneous shape of the sample, but also the lamellar feature of the particles, and the mean face diameter is about 80 nm,

which is significantly smaller than that of the reported [3]. It is seen from Fig. 3b that  $\beta-Ni(OH)_2$  nanosheet shows well hexagonal structure and a single-crystalline nature of the nanosheet (fast Fourier transform (FFT), inset of Fig. 3b). The enlarged detail of a stack side (Fig. 3c) enables the mean thickness of a layer to be estimated at about 15 nm, such as Fig. 3c. The FFT image (inset of Fig. 3c) indicates that it consisted of  $\beta-Ni(OH)_2$  nanosheets with an oriented crystallographic axis along the [0 0 1] direction. The possible chemical composition of the sample was analyzed through the EDS (Fig. 3d). The presence of peaks demonstrates that the nanosheets are composed of Ni, O, small amount of Cu and

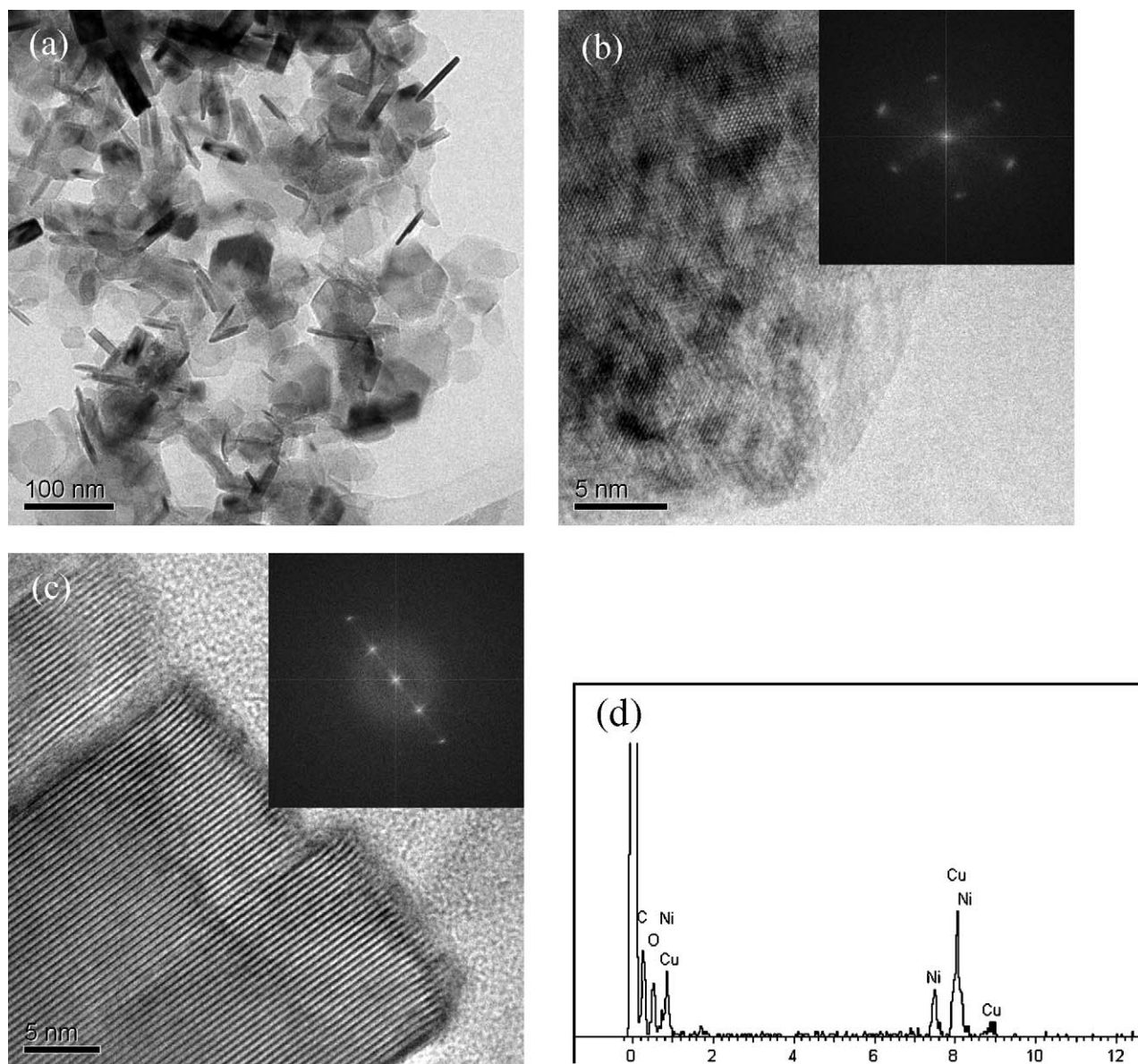


**Fig. 3.** (a) TEM image of sample S3; (b) HR-TEM image of sample S3. The inset is the corresponding FFT. (c) HR-TEM image of sample S3 stack side. The inset is the corresponding FFT. (d) EDS spectrum of sample S3.

C. The copper and carbon signals were due to the supporting copper grid.

All of the film samples deposited with various temperature exhibit similar TG-DSC curves. Fig. 4 shows TG-DSC curves of

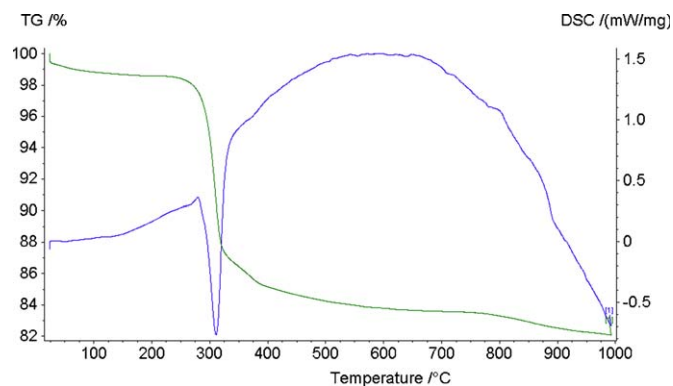


**Fig. 4.** TG and DSC of sample S3.

$\beta$ -Ni(OH)<sub>2</sub> thin film synthesized at 170 °C for 2 h. The  $\beta$ -Ni(OH)<sub>2</sub> underwent multi-step weight losses due to dehydration and decomposition. The initial weight loss of about 1% represented the removal of the physically adsorbed water molecules. The followed weight loss of about 17% is in good agreement with the theoretical weight loss value (19.4%) caused by the decomposition of Ni(OH)<sub>2</sub>. The DSC curve shows only one large endothermic peak. The endothermic peak with the maximum peak located at around 340 °C corresponds to the endothermic behavior during the decomposition from Ni(OH)<sub>2</sub> to NiO. It has been reported that the decomposition of Ni(OH)<sub>2</sub> to NiO occurs between 298 and 342 °C [31,33]. The temperature ranges of the endothermic peak in the DSC curve fits very well with those of the weight loss in the TG curve.

The Ni thin films were obtained by reduction of  $\beta$ -Ni(OH)<sub>2</sub> nanocrystalline thin films. The catalytic activity of Ni thin films can be tested through the absorption of carbon by catalyst from the gas phase and precipitation of carbon to form CNFs. In order to examine the effect of hydrothermal condition catalytic reaction, five catalysts pretreatment with different conditions were studied

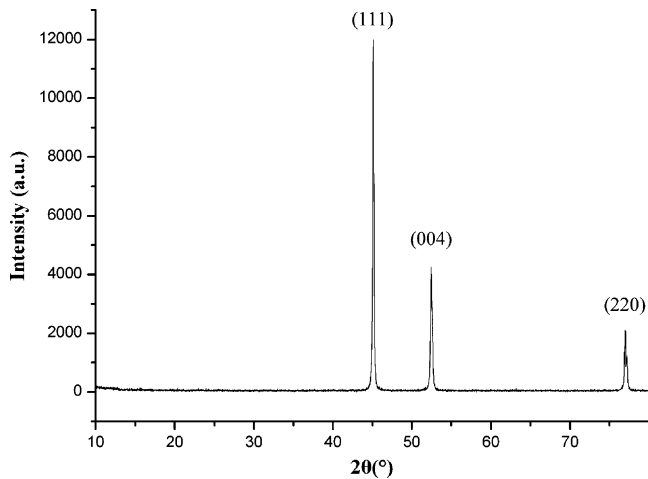


Fig. 5. XRD pattern of the Ni thin film reduction of sample S3.

(as listed in Table 1). As shown in Table 1, the carbon yield slightly increased from 177% to 494% over S1 to S2, respectively. The highest carbon yield, being 1822%, was obtained for S3. Nevertheless, the carbon yield declined to 1611% for S4, and decreased to 1258% over S5. The catalytic activity passes through a maximum at 170 °C for 2 h. From the reaction results of acetylene decomposition, it seems that the hydrothermal temperature of the synthesized Ni(OH)<sub>2</sub> thin film precursors has an important effect

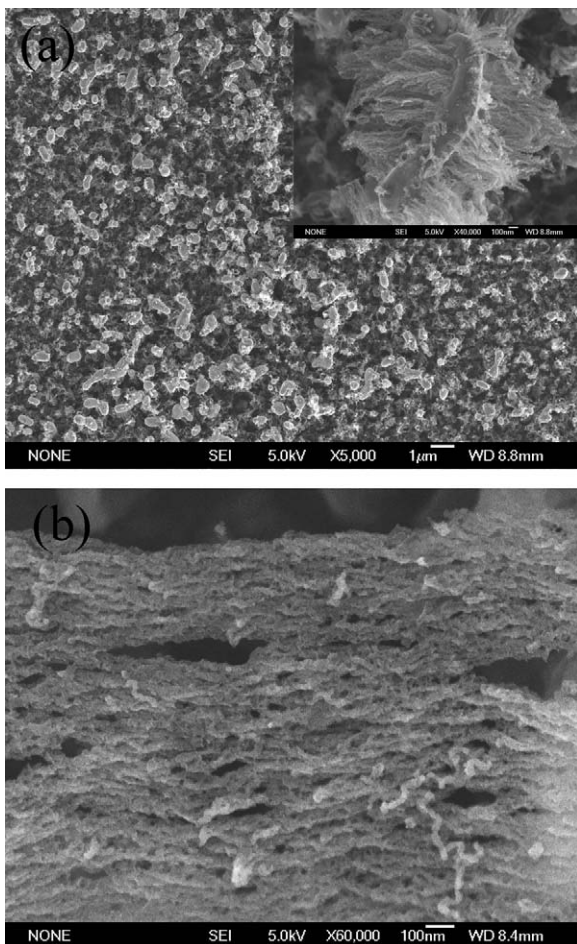


Fig. 6. (a) SEM image of as-grown oriented CNFs on a quartz substrate. The inset is the expanded views of the tip. (b) SEM image of the middle section.

on the catalytic performance of the reduced Ni catalysts. Previous reports has revealed that temperature has influence on the storage capacity, nickel content and weight loss for precipitated Ni(OH)<sub>2</sub> [32–34]. For example, on increasing the temperature of hydrothermal treatment from 60 to 160 °C, the tap density increase from 0.4 to 2.0 g cm<sup>-3</sup>, and wt.% Ni increase from 48.7 to 58.7, and weight loss at 800 °C decreases from 25.4% to 19.7% [33]. The increase in catalytic activity with increase in treatment temperature could be due to increase of Ni content. If the Ni content is increased, carbon storage capacity of Ni would be enhanced after being reduced. Thus the CNFs yield increase remarkably. It is a good agreement with our experiment results.

Ni thin films with the high catalytic activity were obtained by reduction of these Ni(OH)<sub>2</sub> nanocrystalline thin films synthesized at 170 °C for 2 h in hydrothermal condition. XRD measurement was then conducted to follow the evolution of the Ni thin film. Fig. 5 shows that one of the phase is indexed to the (1 1 1), (0 0 4), and (2 2 0) planes of Ni (JCPDS no. 04-0850) with the typical peaks at  $2\theta = 44.5^\circ$ ,  $51.85^\circ$  and  $76.37^\circ$ , respectively. It is revealed that the Ni(OH)<sub>2</sub> nanocrystalline thin films were reduced into Ni thin film

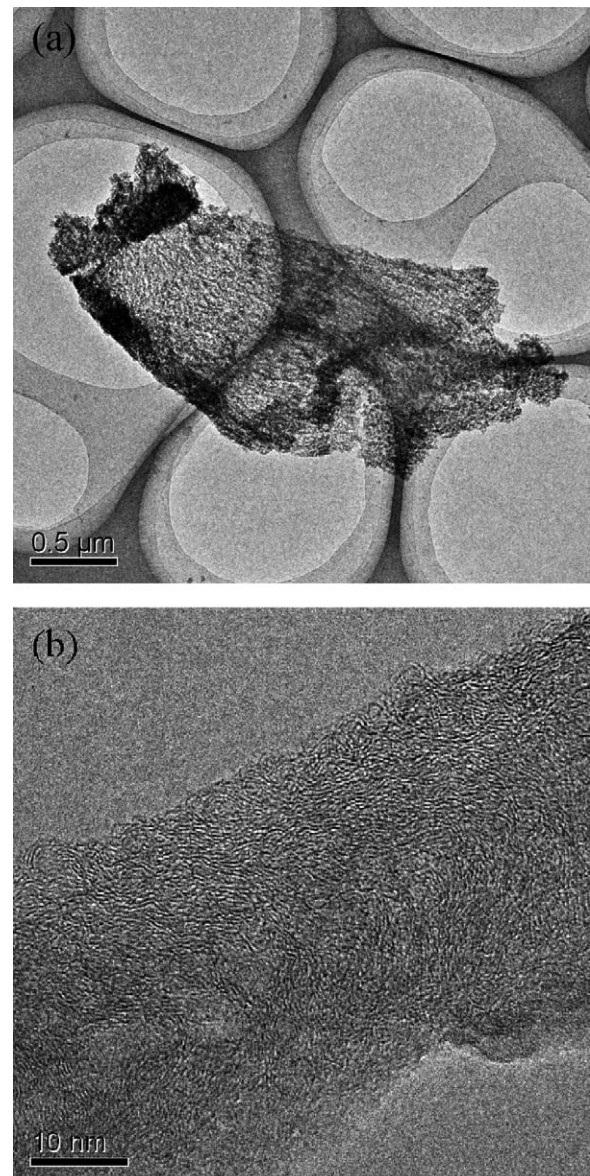


Fig. 7. (a) TEM image of the oriented CNFs; (b) HR-TEM image of the single nanofiber.

on the quartz substrate. For the reduced Ni thin film, the carbons were all in oriented nanofibers form. Fig. 6a displays a SEM image of oriented CNFs growing normal to the quartz substrate. Most of CNFs are approximately perpendicular to the substrate. The magnified SEM image (inset of Fig. 6a) reveals a top view of a bundle surface. Fig. 6b shows section SEM image of the highly oriented CNFs with quite uniform diameter. TEM observations were performed to investigate the morphology of the oriented CNFs sample in detail. Fig. 7a depicts that the nanofibers are generally oriented in one direction to form an array, which are several microns long. The Ni cluster was all located at the tips of CNFs, which is in good agreement with that shown from SEM images. It can clearly be seen that Ni cluster was located at the tips of oriented CNFs. CNFs remained well oriented arrays even after drastic ultrasonic agitation. Fig. 7b shows the single nanofiber has the diameter of about 50 nm. Additionally, the graphitic sheets are waved over a shot range and thus are the most defective structures, and the outer sheets are less crystalline compared with the inner ones. In our experiment, based on the TG-DSC experiment, the calcinations at 400 °C in argon resulted in the decomposition of Ni(OH)<sub>2</sub> thin film to NiO thin film and the in situ conversion of Ni(OH)<sub>2</sub> nanosheets to NiO nanosheets. The NiO nanosheets were reduced in the hydrogen. And with the temperature increasing, Ni nanosheets reformed many larger clusters on the surface of quartz substrate. Large Ni clusters were the result of the sintering or coalescence of the metal atoms and their strong cohesive forces [35,36]. At the growth temperature, these metal catalyst particles had sufficient mobility to coalesce into larger particles. For the large-scale production of CNFs, it is desirable to anchor the metal catalyst firmly to a support to impede the formation of larger catalyst clusters. The interaction of the catalyst with the support can be characterized by its contact angle at the growth temperature, analogous to surfaces. Ni on the quartz substrate has a large contact angle at 750 °C, and the Ni particles were all located at the tips of the oriented CNFs. Thus tip growth is favored in this system.

#### 4. Conclusion

In summary, β-Ni(OH)<sub>2</sub> thin films with unique nanostructure were obtained by hydrothermal method. The thin films were constructed with hexagonal β-Ni(OH)<sub>2</sub> nanosheets. The nanosheet mean diameter was about 80 nm, and the thickness of each sheet was 15 nm. The hydrothermal temperature played an important role in the films growth process and influence on the morphologies and catalytic activity of the catalysts. The optimum hydrothermal condition of β-Ni(OH)<sub>2</sub> thin film as the catalyst precursor in synthesizing oriented CNFs has been found to be 170 °C for 2 h. A yield up to 1822 wt.% was obtained by acetylene cracking on the Ni(OH)<sub>2</sub> precursor. The oriented CNFs were amorphous and uniform diameter of 50 nm.

#### Acknowledgements

This research work is supported by the Creative Research Group of National Science Foundation of China (Grant No. 50721003) and the Foundation of the Ministry of Education of China for Returned Scholars (Grant No. 2005383).

#### References

- [1] T. Neuberger, B. Schopf, H. Hofmann, M. Hofmann, B. von Rechenberg, *J. Magn. Mater.* 293 (1) (2005) 483.
- [2] H. Yang, Q. Lu, F. Gao, Q. Shi, Y. Yan, F. Zhang, S. Xie, B. Tu, D. Zhao, *Adv. Fun. Mater.* 15 (8) (2005) 1377.
- [3] C. Coudun, F.J. Hocheppied, *J. Phys. Chem. B* 109 (13) (2005) 6069.
- [4] E. Jiran, C.V. Thompson, *Thin Solid Films* 208 (1) (1992) 23.
- [5] Y. Li, B. Zhang, X. Xie, J. Liu, Y. Xu, W. Shen, *J. Catal.* 238 (2) (2006) 412.
- [6] T.V. Choudhary, C. Sivadinarayana, C.C. Chusuei, A. Klinghoffer, D.W. Goodman, *J. Catal.* 199 (1) (2001) 9.
- [7] S. Takenaka, H. Ogihara, I. Yamanaka, K. Otsuka, *Appl. Catal. A: Gen.* 217 (1–2) (2001) 101.
- [8] M.A. Ermakova, D.Y. Ermakov, G.G. Kuvshinov, *Appl. Catal. A: Gen.* 201 (1) (2000) 61.
- [9] R.A. Couttenye, M.H. De Vila, S.L. Suib, *J. Catal.* 233 (2) (2005) 317.
- [10] M.C. Diaz, J.M. Blackman, C.E. Snape, *Appl. Catal. A: Gen.* 339 (2) (2008) 196.
- [11] X. Zhang, W. Song, P.J.F. Harris, G.R. Mitchell, T.T.T. Bui, A.F. Drake, *Adv. Mater.* 19 (8) (2007) 1079.
- [12] G. Zhang, C. Fan, L. Pan, F. Wang, P. Wu, H. Qiu, Y. Gu, Y. Zhang, *J. Magn. Mater.* 293 (2) (2005) 737.
- [13] A. Matsuda, S. Akiba, M. Kasahara, T. Watanabe, Y. Akita, Y. Kitamoto, T. Tojo, H. Kawaji, T. Atake, K. Koyama, M. Yoshimoto, *Thin Solid Films* 516 (12) (2008) 3873.
- [14] D.D. Zhao, S.J. Bao, W.J. Zhou, H.L. Li, *Electrochem. Commun.* 9 (5) (2007) 869.
- [15] N. Guoqing, L. Yi, W. Fei, W. Qian, L. Guohua, *J. Phys. Chem. C* 111 (5) (2007) 1969.
- [16] L.H. Yu, C.H. Kuo, C.T. Yeh, *J. Am. Chem. Soc.* 129 (32) (2007) 9999.
- [17] K.Y. Tse, L. Zhang, S.E. Baker, B.M. Nichols, R. West, R.J. Hamers, *Chem. Mater.* 19 (23) (2007) 5734.
- [18] H. Le Poche, J. Dijon, T. Goislard de Monsabert, *Carbon* 45 (15) (2007) 2904.
- [19] D. Deng, J.Y. Lee, *Chem. Mater.* 19 (17) (2007) 4198.
- [20] S.F. Ahmed, S. Das, M.K. Mitra, K.K. Chattopadhyay, *Appl. Surf. Sci.* 254 (2) (2007) 610.
- [21] Y. Li, X. Xie, J. Liu, M. Cai, J. Rogers, W. Shen, *Chem. Eng. J.* 136 (2–3) (2008) 398.
- [22] R. Longtin, C. Fauteux, L.P. Carignan, D. Therriault, J. Pegna, *Surf. Coat. Technol.* 202 (12) (2008) 2661.
- [23] H. Liu, G.A. Cheng, R. Zheng, Y. Zhao, C. Liang, *Surf. Coat. Technol.* 202 (14) (2008) 3157.
- [24] B.K. Lee, G.B. Cho, K.K. Cho, K.W. Kim, Structural and electrochemical evaluation of a Si film electrode fabricated on a Ni buffer layer, *Trans Tech Publications Ltd., Stafa-Zuerich, CH-8712, Switzerland, Jeju, South Korea, 2007*, p. 1011.
- [25] D.J. Kong, Y.K. Zhang, Z.G. Chen, L.H. Zhang, J.Z. Lu, *J. Lasers* 34 (6) (2007) 871.
- [26] G. Nakagawa, T. Asano, M. Miyasaka, *Jap. J. Appl. Phys. Part 1: Regular Papers and Short Notes and Review Papers* 45/5 B (2006) 4335.
- [27] S.-P. Chai, S.H. Sharif Zein, A.R. Mohamed, *Carbon* 45 (2007) 1535.
- [28] A.E. Shalagina, Z.R. Ismagilov, O.Y. Podyacheva, R.I. Kvon, V.A. Ushakov, *Carbon* 45 (2007) 1808.
- [29] K.O.C. De Chen, E. Ochoa-Fernández, Z. Yu, B. Tøtdal, N. Latorre, A. Monzón, A. Holmen, *J. Catal.* 229 (2005) 82.
- [30] D. Wang, C. Song, Z. Hu, X. Fu, *J. Phys. Chem. B* 109 (3) (2005) 1125.
- [31] G.J.d.A. Soler-Illia, M. Jobbagy, A.E. Regazzoni, M.A. Blesa, *Chem. Mater.* 11 (11) (1999) 3140.
- [32] X. Kong, X. Liu, Y. He, D. Zhang, X. Wang, Y. Li, *Mate. Chem. Phys.* 106 (2–3) (2007) 375.
- [33] L.X. Yang, Y.J. Zhu, H. Tong, Z.H. Liang, L. Li, L. Zhang, *J. Solid State Chem.* 180 (7) (2007) 2095.
- [34] R. Acharya, T. Subbaiah, S. Anand, R.P. Das, *J. Power Sources* 109 (2) (2002) 494.
- [35] C. Guo, Y. Zuo, X. Zhao, J. Zhao, J. Xiong, *Surf. Coat. Technol.* 202 (14) (2008) 3385.
- [36] C. Guo, Y. Zuo, X. Zhao, J. Zhao, J. Xiong, *Surf. Coat. Technol.* 202 (14) (2008) 3246.